GA–A26769

ASSESSING MATERIAL MIGRATION THROUGH ^{13}C INJECTION EXPERIMENTS

by
P.C. STANGEBY

JULY 2010

GENERAL ATOMICS

DISCLAIMER

This report was prepared as an account of work sponsored by an agency of the United States Government. Neither the United States Government nor any agency thereof, nor any of their employees, makes any warranty, express or implied, or assumes any legal liability or responsibility for the accuracy, completeness, or usefulness of any information, apparatus, product, or process disclosed, or represents that its use would not infringe privately owned rights. Reference herein to any specific commercial product, process, or service by trade name, trademark, manufacturer, or otherwise, does not necessarily constitute or imply its endorsement, recommendation, or favoring by the United States Government or any agency thereof. The views and opinions of authors expressed herein do not necessarily state or reflect those of the United States Government or any agency thereof.

GA–A26769

ASSESSING MATERIAL MIGRATION THROUGH ^{13}C INJECTION EXPERIMENTS

by
P.C. STANGEBY*

This is a preprint of a paper to be presented at the Nineteenth International Conference on Plasma Surface Interactions, May 24-28, 2010, in San Diego, California, and to be published in the *Proceedings.*

*University of Toronto Institute for Aerospace Studies, Toronto, Canada.

Work supported in part by
Collaborative Research Opportunities Grant from the National Sciences and Engineering Research Council of Canada and the U.S. Department of Energy under DE-FC02-04ER54698

GENERAL ATOMICS PROJECT 30200
JULY 2010

GENERAL ATOMICS

ABSTRACT

To mimic a localized impurity source for materials migration studies, $^{13}CH_4$ has been injected into AUG, DIII-D, JET, JT-60U and TEXTOR at a single location into repeat, well-characterized plasmas, making for much more interpretable data than campaign-integrated erosion and deposition. Such studies have shown convincingly that for single null configurations, material is likely to migrate from the wall to the inner divertor creating tritiated co-deposits there. It has also indicated that for an unbalanced double-null configuration similar to ITER's the sputtered wall material is likely to create codeposits on the blanket wall rather than the divertor; this has implications for ITER tritium retention in Be codeposits since the wall can only be baked to 240°C. The location and magnitude of tritium codeposition in the 1997 JET DTE was not as expected from the 1991 PTE. It is recommended that ^{13}C or other tracer experiments be performed in ITER as early as possible.

I. THE NEED TO UNDERSTAND MATERIAL MIGRATION

Material migration is important because it is net, rather than gross, erosion which is of practical consequence; without material migration, there is no net erosion and no deposit formation. Net erosion and deposit formation are of practical importance because of: (a) wearing away of the plasma facing component (PFC) armour, (b) co-deposition retention of T in low-Z deposits, (c) dust due to exfoliated and spalled deposits, (d) deposition on mirrors, (e) mixed material effects such as the creation of low melting point alloy's e.g. BeW, (f) disruptions caused by exfoliated/spalled material entering the plasma, so-called "UFO's," (g) disruptions caused by the melting of deposits which are proud of power-loaded surfaces, (h) other adverse effects due to buildup of unwanted eroded material at critical locations e.g. metal-bridging of gaps and castellations which can result in cracking of the Cu water channels due to eddy currents and thermal stresses. It is important to know where the deposition occurs: deposition on plasma-facing (rather than plasma-hidden) surfaces is beneficial for recovery of tritium from co-deposits; however, it is potentially harmful regarding dust formation, UFO-induced disruptions, divertor deposition pile-up problems, etc.

In progressing from present fusion devices to reactors, the annual energy load, $E_{load}^{year} \equiv P_{heat}\tau_{annual}$ will increase by ~ 5 orders of magnitude, Table 1, where P_{heat} [MW] is the heating power and τ_{annual} [s/yr] is the annual run time. This is a much greater scaling up than is involved in almost any other aspect required for the development of practical magnetic fusion energy. If the crude assumption is made that gross erosion scales with the energy load, then the rate of gross erosion at the divertor strike points of a reactor could be ~ 5 orders of magnitude higher than in present devices. The measured rate of *net* erosion in present devices is 0.1–10 nm/s [1], thus for a typical 10^4 s/year operation the rate of target surface recession is only $\sim 10^{-6}$–10^{-4} m/year. However, if net erosion were to also scale up by 5 orders of magnitude then for reactors the rate of recession of the divertor targets would be 0.1 – 10 m/year which is not acceptable. Fortunately the plasma conditions foreseen at the divertor targets of devices like ITER and FDF, $T_e \sim$ few eV and $n_e \sim 10^{21}$ m^{-3}, are such as (i) to strongly reduce the gross erosion rates compared with those for average divertor conditions in present tokamaks and also (ii) to strongly suppress net erosion relative to gross erosion by prompt local deposition of sputtered particles: when the ionization mean free path for the sputtered impurity neutral L_{ioniz} is less than the fuel ion larmor radius ρ_{DT}, then the strong E-field in the magnetic pre-sheath (MPS), of thickness $L_{MPS} = 3$–$10\ \rho_{DT}$ [2,3], promptly returns the ionized impurity to the target [4]. For $T_e \sim 5$ eV and $n_e \sim 10^{21}$ m^{-3}, $L_{ioniz} < L_{MPS}$ for both high-Z elements like W and low-Z ones like C. Also for high-Z

elements at these plasma conditions, $L_{\text{ioniz}} < \rho_Z$ (the impurity ion larmor radius), in which case before the ionized impurity has completed one gyro-orbit, it will strike the surface again and be deposited [5].

TABLE 1. Rough estimate of net erosion rate of main walls based on assumptions in text. Assumes 100% wall coverage by Be, B, C or W. Other estimates: * from [6] and ** from [74].

Device	P_{heat} (MW)	τ_{annual} (s/yr)	E_{load}^{year} (TJ/yr)	Beryllium net wall erosion rate (kg/yr)	Boron net wall erosion rate (kg/yr)	Carbon net wall erosion rate (kg/yr)	Tungsten net wall erosion rate (kg/yr)
DIII-D	20	10^4	0.2	0.13	0.11	0.08	0.16
JT 60SA	34	10^4	0.34	0.22	0.19	0.15	0.27
EAST	24	10^5	2.4	1.6	1.2	0.82	1.8
ITER	100	10^6	100	77 [29*]	64	44 [53*]	92 [41*]
FDF	100	10^7	1000	610	500	340	740
Reactor	400	2.5×10^7	10000	6500 [21000**]	5300	3700	7900 [5000**]

Unfortunately the PFCs at the main vessel walls will not benefit from prompt redeposition since the plasma there is much less dense, nor from the first effect, (i), since the average energy of the impacting particles is much higher than at the targets. Therefore at the walls net erosion is likely to be comparable to gross erosion, the latter being due to charge exchange neutrals and (relatively) dilute plasma contact. Table 1 provides rough estimates for the wall erosion rate assuming: (i) physical sputtering by cx neutral tritons only; $E_{T_0}^{cx} = 300$ eV, which is a typical average value calculated for the outer wall in ITER [6-8]; (ii) normal incidence yields [9] doubled to account for surface roughness and ion deflection in the MPS: for (Be, B, C, W), Y^{cx} = (0.083, 0.056, 0.035, 0.0024); (iii) no sputtering included for D_0, He_0 or any plasma-wall contact (ionic); (iv) no chemical sputtering or radiation enhanced sublimation of C at reactor-relevant temperatures, e.g. $T_{wall} \sim 1000$ C [10]; (v) total charge-exchange power loss $P_{cx} = 0.05\ P_{heat}$, which is in the range estimated for ITER [7,8,11], thus $0.025\ P_{heat} = E_{T_0}^{cx}\Phi_{T_0}^{cx}$, where $\Phi_{T_0}^{cx}$ is the particle flux to the walls, thus gross erosion rate = $Y^{cx}\Phi_{T_0}^{cx} \approx$ net erosion rate for the main wall.

In current tokamaks the main wall generally tends to be in a (spatially-averaged) state of net erosion with the lost material being transported to the divertor where it accumulates [12]. Future devices seem likely to need to exploit detachment or semi-detachment in order to reduce target power loads to sustainable levels. In cold, detached conditions in DIII-D the entire divertor – both outer as well as inner targets – are in a state of net deposition due to PFC material migration from the walls [13,14]. It is therefore possible that we have been worrying about the wrong problem. As noted above, there is the potential for intolerable wear rates at the strike points in reactors; however, it

may be that the entire divertor will be in a state of net deposition due to migration of eroded wall material. Because of the large wall area, the wall erosion itself may be tolerable providing it is not highly localized. The problem, however, would then be to clear the PFC slag, i.e. the accumulated material from the walls, out of the divertor rapidly enough to avoid disrupting plasma operation. Our present understanding of material migration is not adequate to be able to reliably anticipate which of these two extremes will occur in future devices nor whether both might occur simultaneously at different locations in the divertor.

II. WHAT WE NEED TO UNDERSTAND ABOUT MATERIAL MIGRATION AND THE AVAILABLE TOOLS

We need to understand material migration occurring on several, very different scale lengths: (a) *local scale* where a critical issue is the effect of prompt local deposition at suppressing net relative to gross erosion, thus on scale lengths down to the larmor radius; (b) *intermediate scale* where migration is due to not only ions but neutrals, thus on scale lengths down to neutral ionization penetration; a key issue here is material migration from one part of a divertor to another part; (c) *long scale*, i.e. the scale of the entire device, where migration is primarily ionic and may not be impurity-specific, particularly; a key issue here is material migration from the main walls to the divertor.

As already noted, in reactors it may be essential that net erosion be greatly suppressed relative to gross erosion and that this can be achieved, in principle, by the processes of prompt, local re-deposition of sputtered material. Although the ideas underlying these processes are so basic that we can scarcely imagine how they could fail to hold, and while there is also evidence for their validity [15–17], there are also indications that something important may be missing in our understanding of the controlling physics here: in C-Mod the measured net erosion rate of Mo at the outer strike point is measured to be about an order of magnitude larger than expected from simple basic considerations and also contrary to detailed WBC code modeling [18]. This may point to a major and critical challenge to our understanding of material migration: identification of controlling physics at the local scale.

The term "diagnosis" is probably assumed by most tokamak physicists to automatically mean (i) *spatially comprehensive*, (ii) *in situ* and (iii) *real time*. Alas, in the field of material migration today we are largely stuck in a diagnostic predicament. It is true that for decades we have been able to measure the net erosion and deposition at all locations — but only at the end of campaigns where the patterns are the integrated result of an enormous range of conditions, some scarcely characterized, like disruptions, making interpretation almost impossible. Quartz microbalances installed in protected cavities facing the plasma can provide local, time–resolved measurements of net erosion and deposition [12]; however, they cannot be placed on the critically important power-receiving surfaces. The injection of isotope-marked tracer impurities, such as $^{13}CH_4$, provides uniquely informative opportunities to monitor and quantify material migration. This technique was pioneered and extensively exploited on TEXTOR [19–35], since finding widespread application on JET [36–48], ASDEX-U [49–58], DIII-D [59–67] and JT-60U [68]. For local scale studies, probes can be employed which can be removed after

a single shot, or a set of repeat, identical shots; subsequent surface analysis using e.g. Nuclear Reaction Analysis (NRA) which can measure ^{13}C in surface layers above the natural isotope ratio $\left(^{13}C/^{12}C = 0.011\right)$, down to extremely thin layers, $\sim 2\times10^{16}$ $^{13}C/cm^2$ [60]. For intermediate and long scale studies it is still necessary to wait until the vessel is opened for prolonged access, e.g. end of a campaign, to retrieve tiles; however, the tracer injection experiments can be carried out on the last day of the campaign using well-controlled, well-diagnosed, repeat, identical shots thus making for a much more tractable problem of interpretation than for campaign-integrated studies. This is still a far cry from the diagnostic capability which is really needed, namely spatially comprehensive, *in situ* and real time (or at least between shots) surface analysis, but it appears to be the best tool we have today. Relative to the latter, isotope-tracer experiments are still non-ideal since they involve ramp-up/down stages of the discharges which may disturb the patterns created in the steady-state. Also isotope tracers usually have to be injected as elements within a molecular gas, e.g. $^{13}CH_4$, and may behave differently than as a sputtered atom. Even when simulating chemical sputtering of carbon, more than one hydrocarbon species needs to be injected since such are involved in chemical sputtering.

We next review some of the $^{13}CH_4$-injection experiments carried out on various tokamaks, specifically focussing on what we have learned from these experiments that is *generally* relevant to impurity migration, rather than being only *carbon-specific*.

III. A BRIEF REVIEW OF SOME $^{13}CH_4$-INJECTION EXPERIMENTS ON VARIOUS TOKAMAKS

Local scale. In TEXTOR small test-limiters made of graphite or tungsten have been used to inject $^{13}CH_4$ [19-35] and $^{13}C_2H_4$ [31]. The deposition efficiency (on the test-limiter) of the ^{13}C is measured to be quite small, of order 1%, but has been successfully modeled using the ERO code assuming zero sticking probability for hydrocarbon, HC, fragments, and an enhanced sputtering yield of $Y \sim 0.15$ for re-deposited C-layers (enhanced compared with that of graphite) [28,33]. Similarly low deposition efficiencies were measured for other tracers, such as SiD_4 and WF_6 [33] and so is evidently not a carbon-specific effect. It is found that surface roughness has a strong effect on the deposition efficiency, increasing it by 3–5 × for rough surfaces compared to smooth [27]; the proposed explanation of this effect, Fig. 1, would appear to indicate why this is not an impurity-specific effect, primarily.

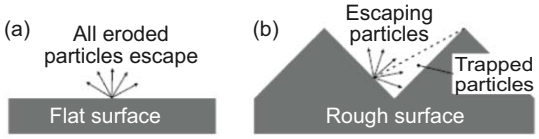

Fig. 1. Illustration of the enhanced prompt re-deposition on rough surfaces [27], reprinted with permission from A. Kreter, et al., Plasma Phys. Control Fusion **50** (2008) 095008.

Local scale. $^{13}CH_4$ injections into the outer divertor in AUG show the effect of both local radial and local poloidal $E \times B$ drifts on local migration [52,53,57]. The $E_{\text{radial}} \times B$ drift downwards (-Z direction) causes a boomerang shape in the ^{13}C deposition pattern on the tiles adjacent to the injection holes while the $E_{\text{poloidal}} \times B$ drift outwards (+R direction) causes the ^{13}C deposition on the upstream side of the hole, both impurity-general effects. The ^{13}C deposition patterns were successfully modeled by the ERO+SOLPS code combination, [53,57], showing that most of the deposition occurred as ions, therefore a basically impurity-general process.

Intermediate scale. In JT-60U ^{13}C injection was used to test the hypothesis that W migrates from outer to inner divertor due to the $E \times B$ drift [68]. A localized set of graphite tiles in the outer divertor, just above the usual strike point location, was replaced with W-tiles (1/21 of the toroidal cicumference) which were then exposed to 2543 shots which, being of various types, therefore made the measured W migration from outer to inner divertor hard to interpret. Measurements of the W deposits on the C-tiles showed that the W did not migrate toroidally primarily but migrated from outer to inner divertor *poloidally* rather than along field lines, raising the question of whether the migration was

due to W-neutrals or poloidal $E \times B$ drift of W-ions. $^{13}CH_4$ was then injected into 13 identical L-mode shots at approximately the same poloidal and toroidal location as the W-tiles. The ^{13}C and W poloidal profiles of deposition on the inner divertor were found to be rather similar, indicating that the W-migration would appear to be due to $E \times B$ ion drift since the neutral transport of C and W are expected to be rather different. It may be noted that the ^{13}C deposition was due to Lmode discharges while the W deposition was due to a variety of discharges; also, the toroidal profiles of deposition differed between W and ^{13}C.

Long scale. Injection of $^{13}CH_4$ near the outer divertor into 31 identical H-mode shots in JET showed that the long path (over the top) to the inner divertor starts near the outer divertor [44,48]. Comparisons of the measured ^{13}C deposition with that calculated using the EDGE2D code indicated that most of the ^{13}C injected just above the outer divertor took the long path over the top of the plasma to the inner divertor, while most of the ^{13}C injected closer to the outer strike point evidently went into the divertor directly, i.e. not by the long path over the top. The JET reciprocating probe, which enters the vessel almost at the top, showed heavier ^{13}C deposition on the side facing the outer divertor than the side facing away. By assuming an imposed parallel force on the C-ions, the EDGE2D simulations were able to reproduce both the locally enhanced ^{13}C deposition at the entrance to the inner divertor (which clearly arrived from over the top of the plasma) as well as the detailed ^{13}C deposition on the probe, even including the effect of erosion of the ^{13}C layer by ongoing plasma exposure. Allowing for the effect of erosion of ^{13}C deposits is difficult in the divertor due to multiple-step erosion and re-deposition but can be more reliable for an isolated object like a probe.

Long scale. In DIII-D it is possible to inject gases such as $^{13}CH_4$ in a way which is truly toroidally symmetric using one or more of the three cryopump plenums (with the cryopumps warm). Gas introduced into these plenums emerges in a toroidally symmetric way into the plasma making for an appreciably more tractable task for experimental interpretation. Distributed, non-local injection is also appreciably less likely to perturb the local plasma than small orifice injection; the opening from the lower pumping plenum to the main vessel in DIII-D is 0.034 m high and extends continuously over $2\pi R \sim 9$ m, thus creating a gas entrance area of ~ 0.3 m^2; the injection rate in the 2008 experiment, see below, was 7×10^{20} $^{13}CH_4$/s, giving an influx density $\sim 2 \times 10^{21}$ $^{13}C/m^2/s$ which is 2-4 orders of magnitude smaller than the influx densities involved in the small orifice injections more generally used.

In 2003 $^{13}CH_4$ was injected into the top of 22 repeat lower single null, low density Lmode shots, with 29 graphite tiles removed for measurements of the surface layers of ^{13}C and the contained D, by NRA and PIGE [59–63]. In 2005 a similar experiment was carried out with injection into the top of 17 repeat, lower single null, high density, H-mode shots, with 64 graphite tiles removed for measurements [64–66]. In both

experiments $\sim 50\%$ of the injected ^{13}C was found in the surface layers which were shown to be toroidally symmetric. In both experiments the thickest deposits were found in the lower divertor (see Fig. 4 of [64]) with very similar deposition on the inner divertor. In both experiments there was ~ no deposition in the outer divertor. The deposition patterns in both experiments were well reproduced using the interpretive OEDGE code [62,65], providing empirical quantification of parallel and cross-field migration velocities and diffusivities as well as identification of some of the physics controlling the material migration including volume recombination and, apparently, a pinch force in the inner SOL operating in the + R-direction.

Over the past decade a "standard" picture has been established of mass transport in the edge based on experiments in AUG, DIII-D, JET and JT-60 [12]: *"In recent years, a general qualitative understanding has been reached about the major pathways of material migration in divertor tokamaks. Main chamber wall components have been identified as the major source of material erosion. The eroded material is transported by scrape-off layer flows, in the case of the ion grad-B drift pointing towards the X-point, predominately towards the inner divertor leg, where it is deposited in the form of amorphous layers."* Because of the toroidal symmetry, the low influx density and the high fraction found of the injected ^{13}C (~ half), the DIII-D injection experiments have provided particularly clear and definitive evidence for the standard picture. The latter, however, is based exclusively on experiments in single null magnetic configurations. ITER, on the other hand, will employ an unbalanced double null configuration with a secondary divertor at the top and the resulting plasma-"wall" interaction will occur primarily at the secondary outer divertor beryllium "target." For this configuration it is not evident that the sputtered Be will, in fact, migrate to the lower, primary divertor but may deposit on the main wall near the top. As discussed above, injection of $^{13}CH_4$ near the outer strike point in *single* null discharges in AUG [52,53,55,57] and JET [44,48] have shown that much or all of the ^{13}C is deposited in the divertor, so it might be anticipated that injection near the outer strike point of the secondary divertor in a *double* null discharge would *not* result in the standard picture of transport to the primary divertor. This would, however, have major practical implications for tritium control since thermal release of tritium from Be co-deposits at the main wall bake temperature in ITER, 240°C, is only partial, 20%60%, in contrast with ~ 85% at the primary divertor bake temperature, 350°C [69]. Therefore in 2008 a third $^{13}CH_4$ experiment was performed in DIII-D, using an unbalanced double null configuration [67]. Because the boundary diagnosis is more complete at the bottom of DIII-D, the magnetic configuration was inverted relative to ITER's, i.e. with the secondary divertor being at the bottom and with the $^{13}CH_4$ being injected using the lower outer cryoplenum (Fig. 2); ion grad-B drift was toward the primary divertor as is the norm. Measured secondary strike point plasma conditions were $n_e = 1 \times 10^{19}$ m^{-3} and $T_e = 10$ eV, which are close to those

projected for the secondary separatrix in ITER, i.e. $0.5-1.5\times10^{19}$ m^{-3} and 10-20 eV [11]. This injection of $^{13}CH_4$ into the outer secondary divertor, mimicking the sputtering of Be at that strike point, resulted in a ^{13}C deposition pattern radically different than for the injections into the top of LSN configurations: while a small fraction migrated across the secondary separatrix into the main SOL and was deposited on the primary (upper) inner target, by far the highest surface concentration of ^{13}C occurred in the secondary, outer divertor close to the injection point. The implications for ITER, as noted, would appear to be significant.

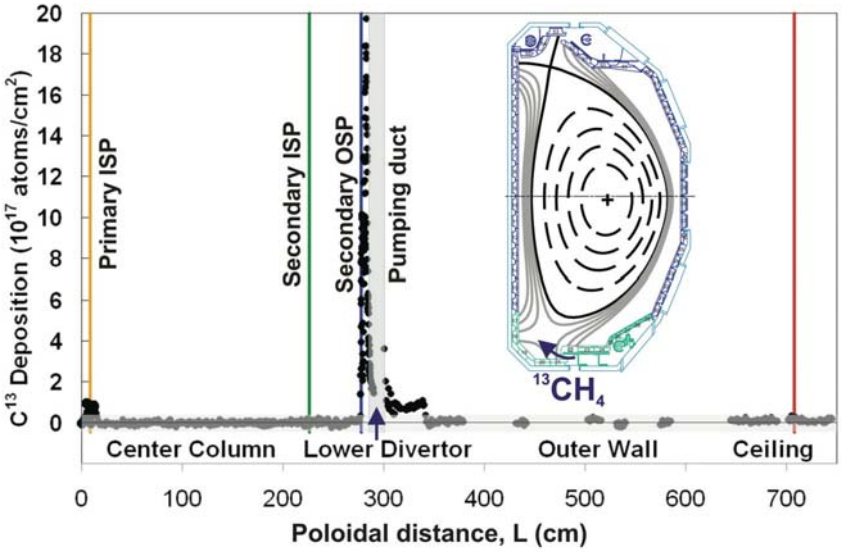

Fig. 2. DIII-D. The injection of $^{13}CH_4$ into the outer secondary divertor of an unbalanced double null configuration, mimicking the sputtering of Be at that strike point. Almost no deposition occurred in the primary divertor and by far the highest surface concentration of ^{13}C occurred in the secondary, outer divertor close to the injection point [67].

Despite the very low influx density employed, $\sim 2\times10^{21}$ $^{13}C/m^2/s$, the local plasma was somewhat perturbed by the gas injection. An increase of D_α of roughly 10% was seen on the chord viewing the plasma closest to the plenum opening (the D_α emission near the secondary divertor strike point did not change nor did T_e as measured by target probes).The OEDGE interpretive analysis [67] included the effect of an extra hydrogen fueling source locally which resulted in frictional transport of some C-ions along the secondary SOL away from the target reducing local deposition and transporting some ^{13}C out of the divertor.

The 1997 JET DTE (Deuterium Tritium Experiment) [70,71] has probably been the most important materials migration experiment in magnetic fusion energy research to date. It was also a tracer experiment similar to $^{13}CH_4$ experiments in all essential aspects: (i) injection of a known amount of a readily measured isotope otherwise not

significantly present in the vessel, (ii) specific plasma conditions (iii) removal of tiles to search for the tracer. The tritium retention was a major surprise, being radically different in both its location and magnitude (much higher) than in the 1991 JET Preliminary Tritium Experiment (PTE) [72]. The purpose of PTE was to anticipate and prepare for DTE and, at the time, it was thought to have achieved that [72]: "*The data obtained (in PTE) have enabled us to get a much better understanding of the principle processes that occur with tritium. This should enable the behaviour of tritium in the next tritium phase of JET (DTE) to be predicted with some confidence.*" Unfortunately this turned out not to be the case. The difference between the measured and predicted inventories increased during the DTE campaign. By the end of plasma operation the measured inventory was $\sim 3.5\times$ greater than predicted from PTE. After the application of various recovery methods the tritium inventory at the end of the DTE campaign was $\sim 17\%$ of the total tritium input to the torus, compared with $\sim 3\%$ for PTE, a factor of $\sim 5.5\times$ difference. The location and nature of the tritiated carbon co-deposits was also entirely different: in PTE they were largely on plasma-facing tile surfaces distributed around the torus; in DTE they were highly concentrated in the lower inner divertor, as thick coatings on water-cooled louvers, much of which had exfoliated and fallen to the bottom of the vessel, out of easy access. The explanation for the radical differences between PTE and DTE has gradually emerged although the story may still be incomplete. PTE employed a completely open divertor at the top of the vessel: the strike points were simply placed on the graphite wall tiles. In DTE the specially installed water-cooled MkIIa divertor at the bottom of the vessel was used. Thus, in PTE there were no significant hidden surfaces out of plasma-contact while in DTE, large cavities in the lower divertor, part of the pumping system, directly faced the targets. In PTE the ambient wall temperature was $300°C$ while in DTE the water-cooled louvers inside the cavities were at $40°C$. Because of the open structure, in PTE there was also strong plasma heating of the co-deposits but almost none in DTE; evidently closely related: recovery of tritium by disruptions was effective in PTE but not in DTE. In PTE the co-deposits were measured to have a low D/C ratio, ~ 0.1 while in DTE they were quite hydrogenated, D/C ~ 0.8.

Had the tritium co-deposition behaviour encountered in DTE been anticipated then various actions might have been taken in advance, including simple house-keeping ones such as arranging for heatable "catchers" to be placed under the water-cooled louvers to collect the exfoliated tritiated material for localized baking, or just removal from the vessel. In PTE most of the retained T was on the regular wall tiles. If a $^{13}CH_4$ experiment had been carried out employing plasma conditions close to those expected for DTE, almost none of the ^{13}C would have been accounted for on the wall tiles but, it may be speculated, the missing ^{13}C would have eventually been found on the louvers. While, in principle, it is possible to obtain the same information using non-tracer techniques there is nothing like introducing a known amount of a readily detectable substance then

hunting it down. If it can't be found initially then efforts will almost certainly be made until it is found. Other materials migration techniques tend not to identify the problem so directly.

It is important to extract the appropriate lessons from this JET landmark materials migration experience to apply to ITER. The ITER wall structure is modular, consisting of ~ 440 individual blanket modules, separated from each other by large gaps, as required for remote maintenance. These gaps present many m^2 of recessed area facing the plasma where tritiated Be co-deposits can accumulate out of direct contact with plasma. Some of the recesses have a high aspect ratio, being wide but not deep, e.g. at port openings, and so access e.g. by flash heating or by controlled disruptions, may be effective at tritium recovery. Other recesses, however, have low aspect ratio, being narrow and deep, for example the 14 cm gaps between the blanket modules which extend ~ 0.5 m radially. It would seem advisable that $^{13}CH_4$, or other suitable tracer, experiments be performed on the ITER wall as soon as this becomes possible.

IV. DISCUSSION AND CONCLUSIONS

The first essential task in tokamak materials migration research is to empirically establish the migration routes, e.g. where do impurities end up which entered the plasma at a specified location? Here ^{13}C injection experiments have been uniquely informative. Injections into the top of single null plasmas have shown long-range transport to the inner divertor, apparently consistent with Mach probe measurements of very fast parallel plasma flow from the low field side to the high field side (for ion grad-B drift toward the divertor). It is not evident, however, that the migration pattern of the recycling fuel plasma, i.e. that measured by Mach probes, is necessarily the same as for non-recycling impurities. In fact experimental conditions are reported in DIII-D where the D-ions and C-ions move in the parallel direction oppositely [73]. Since the point is to identify *impurity* migration routes, it is an important aspect of this technique that actual impurities are tracked.

This basic and essential mapping exercise remains significantly incomplete, a consequence of the fact that such experiments can only be done every year or so on a given tokamak. Migration routes may depend on discharge type, $\bar{n}_e$, P_{heat}, ELM properties, wall gaps, etc, but there is little information on this as yet. It seems plausible that, to zeroth order the long scale migration routes are not impurity-specific but this key question is unaddressed at present. It is evident from the most recent $^{13}CH_4$ experiment on DIII-D that the magnetic configuration — e.g. single- vs unbalanced double-null — can have a profound effect on the material migration overall pattern.

As noted earlier, tracer impurity injection is by no means a perfect tool for studying material migration due to the inability to separate the effects of ramp-up/down from steady phases of discharges, injection as a molecule rather than as a sputtered atom, potential perturbation of the local plasma, etc. Therefore other migration diagnostics including QMBs and campaign-integrated surface analysis remain essential compliments.

Material migration is a major concern, with a number of potential show-stoppers implicated for future DT power devices such as ITER. Beyond ITER the situation looks yet more serious because of the far larger mass of material involved, see table. After the rather comprehensive failure to anticipate the most important materials migration experiment in magnetic fusion research to date — the JET DTE — it is clear that our understanding of material migration is unacceptably weak. There are few tools in our kit. Trace injections such as ^{13}C appear to be the best tool we have today for establishing the whole-vessel picture. The rate of generation of information is very slow because experiments involving the removal of tiles can only be done infrequently. What is really

needed is *in situ*, real time — or at least between discharges — surface diagnosis of the entire inside of tokamaks. Until such diagnostic capability is available tracer experiments will remain indispensible. Their high cost, in time and labour, can make them a challenge to justify. The cost of not doing them can, however, be higher.

REFERENCES

[1] D.G. Whyte, Fusion Sci. Technol. **48**, 1096 (2005).

[2] R. Chodura, Phys. Fluids **25**, 1626 (1982).

[3] P.C. Stangeby and A.W. Leonard, to be submitted to Nucl. Fusion (2010).

[4] J.N. Brooks, Phys. Fluids **B2**, 1858 (1990).

[5] D. Naujoks, *et al.*, Nucl. Fusion **36**, 671 (1996).

[6] A.S. Kukushkin, ITER_D_27TKC6, 14 April 2008.

[7] V. Kotov, *et al.*, J. Nucl. Mater. **390-391**, 528 (2009).

[8] V. Kotov, private communication (2010).

[9] W. Eckstein, "Calculated Sputtering, Reflection and Range Values," IPP 9/132, 2002.

[10] P.C. Stangeby, 2000 "The Plasma Boundary of Magnetic Fusion Devices," Institute of Physics, Bristol, Secs. 3.3.2, 3.3.4.

[11] "Heat and Nuclear Load Specifications for ITER," ITER_D_2LULDH v2.3, 201.

[12] A. Kreter, *et al.*, J. Nucl. Mater. **390-391**, 38 (2009).

[13] W.R. Wampler, *et al.*, J. Nucl. Mater. **290–293**, 346 (2001).

[14] D.G. Whyte, *et al.*, Nucl. Fusion **41**, 1243 (2001).

[15] K. Krieger, *et al.*, J. Nucl. Mater. **266-269**, 207 (1999).

[16] K. Krieger, *et al.*, J. Nucl. Mater. **241-243**, 684 (1997).

[17] D. Naujoks, *et al.*, J. Nucl. Mater. **210**, 43 (1994).

[18] J.N. Brooks, *et al.*, these proceedings, P2-37.

[19] U. Kögler, *et al.*, J. Nucl. Mater. **241-243**, 816 (1997).

[20] A. Kirschner, *et al.*, J. Nucl. Mater. **290-293**, 238 (2001).

[21] P. Wienhold, *et al.*, J. Nucl. Mater. **290-293**, 362 (2001).

[22] M. Rubel, P. Wienhold, D. Hildebrand, Vacuum **70**, 423 (2003).

[23] M. Rubel, *et al.*, J. Nucl. Mater. **329-333**, 795 (2004).

[24] M. Rubel, P. Coad and D. Hole, Vacuum **78**, 255 (2005).

[25] A. Kreter, *et al.*, Plasma Phys. Control. Fusion **48**, 1401 (2006).

[26] A. Kreter, *et al.*, J. Nucl. Mater. **363-365**, 179 (2007).

[27] A. Kreter, *et al.*, Plasma Phys. Control. Fusion **50**, 095008 (2008).

[28] S. Droste, *et al.*, Plasma Phys. Control. Fusion **50**, 015006 (2008).

[29] K. Ohya, *et al.*, J. Nucl. Mater. **390-391**, 72 (2009).

[30] K. Ohya and A. Kirschner, Phys. Scr. **T138**, 014010 (2009).

[31] S. Brezinsek, *et al.*, Phys. Scr. **T138**, 014022 (2009).

[32] R. Ding, *et al.*, Plasma Phys. Control. Fusion **52**, 045005 (2010).

[33] A. Kirschner, *et al.*, these proceedings, I-16.

[34] R. Ding, *et al.*, these proceedings, P3-78.

[35] A.G. Esser, *et al.*, these proceedings, P3-87.

[36] J.D. Strachan, *et al.*, Nucl. Fusion **43**, 922 (2003).

[37] J. Likonen, *et al.*, Fusion Eng. Design **66-68**, 219 (2003).

[38] J.D. Strachan, *et al.*, Nucl. Fusion **44**, 772 (2004).

[39] A. Kirschner, *et al.*, J. Nucl. Mater. **328**, 62 (2004).

[40] J.D. Strachan, *et al.*, J. Nucl. Mater. **337-339**, 25 (2005).

[41] R. Pitts, *et al.*, Plasma Phys. Control. Fusion **47**, B303 (2005).

[42] J.P. Coad, *et al.*, Nucl. Fusion **46**, 350 (2006).

[43] J.P. Coad, P. Andrew, S.K. Erents, J. Nucl. Mater. **363-365**, 287 (2007).

[44] J.D. Strachan, *et al.*, Nucl. Fusion **48**, 105002 (2008).

[45] J.D. Strachan, *et al.*, J. Nucl. Mater. **390-391**, 92 (2009).

[46] M.I. Airila, *et al.*, Phys. Scr. **T138**, 014021(2009).

[47] M.I. Airila, *et al.*, these proceedings, P3-71.

[48] J. Likonen, *et al.*, these proceedings, P3-74.

[49] R. Pugno, *et al.*, J. Nucl. Mater. **337-339**, 985 (2005).

[50] E. Vainonen-Ahlgren, *et al.*, J. Nucl. Mater. **337-339**, 55 (2005).

[51] E. Vainonen-Ahlgren, *et al.*, J. Nucl. Mater. **363-365**, 270 (2007).

[52] R. Pugno, *et al.*, J. Nucl. Mater**. 390-391**, 68 (2009).

[53] L. Aho-Mantila, M. Wischmeier, M. Airila, Contrib to Plasma Phys (2009).

[54] A. Xuereb, *et al.*, submitted to J. Nucl. Mater.

[55] L. Aho-Mantila, *et al.*, Phys. Scr. **T138**, 014019 (2009).

[56] A. Hakola, *et al.*, Plasma Phys. Control. Fusion **52**, 065006 (2010).

[57] L. Aho-Mantila, *et al.*, these proceedings, O-29.

[58] T. Makkonen, *et al.*, these proceedings, P2-28.

[59] S.L. Allen, *et al.*, J. Nucl. Mater. **337-339**, 30 (2005).

[60] W.R. Wampler, *et al.*, J. Nucl. Mater. **337-339**, 134 (2005).

[61] A.G. McLean, *et al.*, J. Nucl. Mater. **337-339**, 124 (2005).

[62] J.D. Elder, *et al.*, J. Nucl. Mater. **337-339**, 79 (2005).

[63] M. Groth, *et al.*, Phys. Plasmas **14**, 056120 (2007).

[64] W.R. Wampler, *et al.*, J. Nucl. Mater. **363-365**, 72 (2007).

[65] J.D. Elder, *et al.*, J. Nucl. Mater. **363-365**, 140 (2007).

[66] J.D. Elder, A.G. McLean, P.C. Stangeby, J. Nucl. Mater. **390-391** (2009) 376.

[67] J.D. Elder, these proceedings, P3-73.

[68] Y. Ueda, *et al.*, Nucl. Fusion **49**, 065027 (2009).

[69] R.P. Doerner, *et al.*, Nucl. Fusion **49**, 035002 (2009).

[70] M. Keilhacker, M.L. Watkins, JET Team, J. Nucl. Mater. **266-269**, 1. (1999)

[71] P. Andrew, *et al.*, J. Nucl. Mater. **266-269**, 153 (1999).

[72] P. Andrew, *et al.*, Nucl Fusion **33**, 1389 (1993).

[73] M. Groth, *et al.*, Nucl. Fusion **49**, 115002 (2009).

[74] K Lackner, EU EFP Workshop on Tungsten. Velence, Hungary, Dec. 7-9 2009.

ACKNOWLEDGMENTS

This work was supported by Collaborative Research Opportunities Grant from the National Sciences and Engineering Research Council of Canada and the US Department of Energy under DE-FC02-04ER54698.